

Vehicular Visible Light Communication with Dynamic Vision Sensor: A Preliminary Study

Wen-Hsuan Shen, Po-Wen Chen, and Hsin-Mu Tsai
 Department of Computer Science and Information Engineering
 National Taiwan University, Taipei 10617, Taiwan
 Email: {d06922019, b05902117, hsinmu}@csie.ntu.edu.tw

Abstract—State-of-the-art vehicular visible light communication (V²LC) systems utilize either a photodiode or a camera as the receiver, while both have their drawbacks. A photodiode-based receiver lacks the capability to separate signals from sources transmitting at the same time and is more vulnerable to interference. On the other hand, a camera-based receiver suffers from low system throughput, resulting from the low image frame rate of commodity cameras. In this paper, we investigate a solution which attempts to combine the best of both, and mitigate their drawbacks. We propose to use a new type of CMOS vision sensor: a dynamic vision sensor (DVS). Instead of recording still frames, a DVS only generates outputs when it senses a significant change of brightness in a pixel. The output of a DVS is a stream of events on the pixel basis with $1 \mu\text{s}$ resolution, which greatly increase the bandwidth. We investigate the key requirements of the modulation wave form when using a DVS camera-based receiver, and propose a new pulse wave form that maintains the same average luminance level while extending the operational range of the system. Preliminary experimental results show that the proposed wave form nearly triples the range to 8 m, compared to the range of 3 m when using the conventional inverse pulse position modulation wave form.

I. INTRODUCTION

Vehicular visible light communication (V²LC) has drawn more and more attention from both academia and industries thanks to the unique advantages offered by visible light communications (VLC). First, the ubiquity of LED devices allows a simple and cost effective way to enable communications on vehicles or in the infrastructure. Only a simple customized LED driver is needed to transform existing lighting on vehicles into a dual functionality (i.e., communication and illumination) device. Second, VLC features highly directional and line-of-sight optical propagation, leading to reduced interference from neighboring vehicles even in dense traffic. However, current state-of-the-arts face great challenges to provide robust communications with a long operation range and with simultaneous transmissions.

V²LC systems can be categorized by the receiver component [1]: photodiode-based systems and camera-based systems. Recent works have demonstrated that photodiode-based systems deliver a communication range of 40-50 m [2], [3]. However, a photodiode combines all incoming

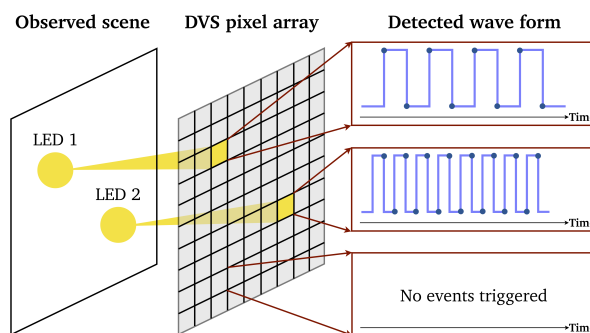


Fig. 1. Illustration of the operation of DVS. Instead of reporting pixel intensity regularly at a fixed sampling rate, each pixel only reports an ON or an OFF event when a significant change of intensity is detected. Those without significant change of intensity would generate no output at all.

light within a wide field-of-view (FOV) angle into one aggregated signal. This creates difficulty in separating signals coming from multiple sources. Moreover, ambient interference, such as sunlight or other luminaries in the environment, would also be captured. These limits the range of the photodiode-based systems. One way to deal with this particular issue is to narrow the FOV of the system, e.g., to $\pm 10^\circ$ [2], in order to reduce the captured interference. However, this is not feasible for V²LC, as even small amount of mobility would result in misalignment between the transmitter and the receiver and, in turn, link outage.

On the other hand, the high spatial resolution of camera-based systems allows the receiver not only to differentiate multiple transmitting sources, but also to filter out unwanted light sources or interference at different spatial locations. In addition, camera-based systems offer a wide FOV, which can accommodate a good amount of mobility. However, the greatest limitation of camera-based systems is the low temporal resolution (typically 30-120 frame per second), resulting in low system throughput [4]. Past works making use of frame-based commodity cameras have shown to deliver only short communication range and a low data rate of a few Kbps [5], [6]. Furthermore, the high computing requirements limit the communication performance. There were also efforts making use of high-speed

or special-purposed cameras, which provide improvement in data rate and communication range [7]–[9] yet at higher cost.

This paper presents an effort to strike a balance between the capability to spatially filter out interference and high system throughput. We propose to implement the receiver with a special vision sensor called dynamic vision sensor (DVS) [10]. As shown in Figure 1, unlike a conventional frame-based camera, a DVS camera only reports change-of-intensity events. The camera only generates output when such events occur. No absolute pixel intensity is reported. This allows the precious output bandwidth to be reserved for information-carrying and thus time-varying signal captured by the camera. Moreover, DVS features a much larger dynamic range of 120 dB [11] compared to conventional cameras¹. This wide dynamic range allows DVS to demonstrate great resilience to strong light sources such as bright sunlight up to 100 klux [10], [12]. These unique characteristics reveal a great opportunity to provide higher system throughput at longer range while preserving the advantage of camera-based systems - their spatial filtering capability. Finally, as DVS only reports changes in intensity, fixed image background is naturally filtered out and the amount of computation required to process the camera output is greatly reduced.

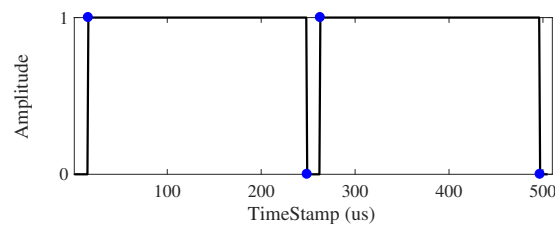
In this paper, we present a preliminary study investigating the potential of using DVS as the VLC receiver. In section II, we first give a brief introduction of DVS cameras, and highlight special properties which may have impacts on the communication performance of a DVS-based VLC system. Then, in section III, we outline two key requirements as a guide to select proper modulation wave forms used with a DVS. According to these requirements, we further propose a new wave form which well suits the characteristics of a DVS and extends the communication range while maintaining a low average luminance level. Finally, we present our implementation and some preliminary evaluation results in section IV and section V, before concluding the paper and listing a few future directions in section VI.

II. BACKGROUND - DYNAMIC VISION SENSOR

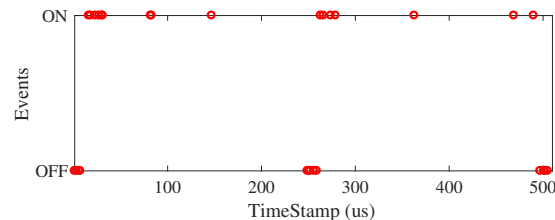
Nowadays, the concept of *frame*, i.e., reporting the intensity value of every pixel at a constant rate, has been taken for granted when considering a typical camera. Nevertheless, the presence of “frame” becomes a bottleneck of the communication throughput. A typical approach to deliver high throughput is to make use of a camera with high frame rate. This, however, results in higher implementation cost and higher amount of computation.

The key reason for such bottleneck is that *much of what is reported in the frame is not relevant to the transmitted information*. Information is usually represented by the

¹As a data point, Sony RX100 mark 6, an off-the-shelf premium consumer pocket camera, has a dynamic range of 36 dB.



(a) The events which would be generated theoretically, represented by the blue dots.



(b) The actual events that are generated and observed in our implementation, represented by the red circles.

Fig. 2. An example of events generated by DVS, triggered by a square wave (93.6% duty cycle).

changes, not those which stay stationary. As a result, most computations to process the frames are wasted.

In contrast to this, a DVS is an asynchronous vision sensor which outputs a stream of events instead of still frames. Another unique property of DVS is that it only responds to the change in luminance rather than absolute illumination. Pixels in a DVS work independently and asynchronously from each other. Rather than continuously sampling and processing unchanged values, the pixels within the image sensor monitor the incoming photocurrent which is then converted into a voltage. The latest incoming voltage is compared to the last sampled voltage, and, if the difference between these two voltages is larger than a certain threshold, an event is triggered by the observing pixel. This triggered output is in the form of address-event representation (AER) which encodes the address of the pixel capturing the change and the polarity of the change (ON or OFF). The address here is represented as the x , y coordinates of the pixel array while the polarity means the sign of the difference. An ON event implies that the observed luminance is increasing, whereas an OFF event implies a decreasing change of luminance.

Theoretically, a DVS generates *one* event when one of its pixels senses a luminance change. Take a blinking LED for example, the DVS would output one *ON* event as the LED switched on, and one *OFF* event as the LED switched off. Therefore, as shown in Figure 2(a), if an LED emits a square wave, there should be two events per cycle at any given frequency. In reality, however, the events are generated with a minimum latency of 12 μ s [11], and for more than once. This is shown in Figure 2(b). Both the latency and the number of generated events depend on the bias setting of the DVS, as well as the distortion of the

transmitted wave form due to the parasitic capacitance of the transmitting LED component.

One can observe that there are a number of ON and OFF events after the rising and the falling edges of the transmitted square wave, respectively. Furthermore, the triggered events do not form an accurate square wave and thus a post-processing algorithm is needed to reconstruct the transmitted wave form (see section IV-C). In addition, we also find an interesting phenomenon as follows. There are a number of residual ON events which appear long after the rising edges. On the other hand, OFF events appear as expected, only right after the falling edges. This phenomenon has constantly been observed throughout the experiments, and thus, we take this into consideration when designing the new wave form.

III. MODULATION WAVE FORM

Our next objective is to investigate the key requirements of the wave form design, based on the characteristics of DVS. These would have great impact on the performance of a DVS-based VLC system. Then, we analyze three conventional VLC wave forms based on these requirements as benchmarks. Finally, we propose and present a wave form that is more well suited to DVS.

A. Key requirements of the wave form

Large time variation. DVS only generates events when there is a significant change of received intensity over a short period of time. Note that the transmitted wave form needs to be reconstructed from the generated ON and OFF events at the receiver. Therefore, to allow reliable and correct detection, the transmitted wave form needs to have a number of sharp transition(s), i.e., large change of its intensity over a short period of time.

Small number of large variations. One key constraint of DVS is that it only allows a certain number of events to be reported over a fixed period of time. This is due to the output bandwidth limit of the sensor. For example, the DVS used in our implementation allows a maximum of one million events per second to be reported. If the number of generated events is larger than this value, some of the events will be dropped and not observed at the output. To allow higher symbol rate, which in turn resulting in higher system throughput, the wave form should minimize the number of sharp transitions per symbol.

Based on these two requirements, we first conclude that the use of a square wave would be better than a sine wave. First, the former has sharp transitions, which allows robust detection at the receiver. Second, the former has a much less number of changes in its intensity than the latter. Based on this analysis, in the following we will only consider square waves as the basis of the employed modulation wave form.

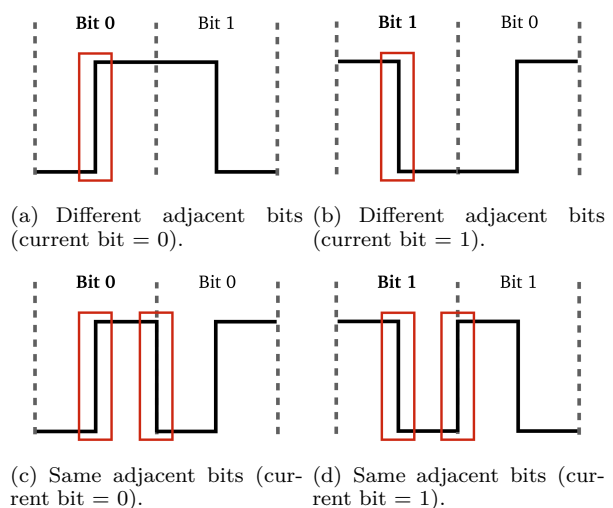


Fig. 3. Four cases of bit permutation in OOK.

B. Analysis of conventional wave forms

We next examine the system performance when using conventional modulation schemes that are often utilized in VLC systems. The goal is to see whether they are also suitable for DVS-based VLC systems.

We investigated three conventional modulation schemes: on-off keying (OOK) with Manchester encoding, inverse pulse position modulation (i-PPM), and frequency shift keying (FSK) as representatives for amplitude shift keying (ASK) and frequency shift keying (FSK). The reason of using i-PPM instead of PPM is that we would like to preserve the main functionality of the LED, illumination. Using PPM with short (positive) pulse width would result in a very low average luminance level, while i-PPM would not.

For fair comparison, we assume that these three wave forms would have the same average output intensity, and the difference between the ON levels and the OFF levels are also the same. Subsequently, there remains only one requirement to fulfill: finding a wave form generating the least number of events per symbol, which implies the highest system throughput.

In this subsection, we start with the derivation of the expected number of generated events per symbol for different modulation schemes. This avoids practical factors such as the bias setting of DVS, the parasitic capacitance of the LED, etc., to affect the results, and provides us a basic understanding of the performance of conventional modulation schemes. Based on the developed formulas, numerical results are produced and presented in section V-A.

OOK with Manchester coding. The wave form can be described in a general form, as a function of time and given by

$$s_i(t) = \begin{cases} \text{sgn}(\sin(\frac{t}{T})), & \text{for symbol 1 (i=1);} \\ -\text{sgn}(\sin(\frac{t}{T})), & \text{for symbol 0 (i=0),} \end{cases} \quad (1)$$

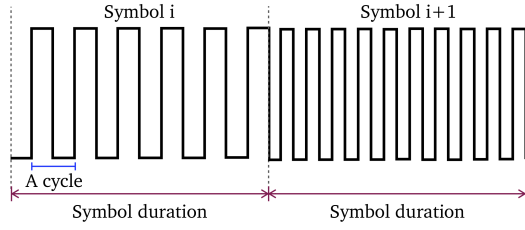


Fig. 4. The wave form of FSK.

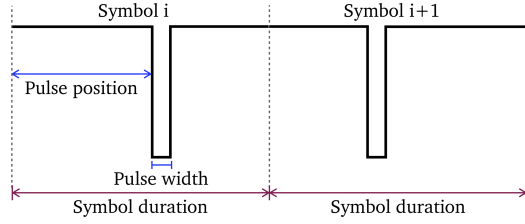


Fig. 5. The wave form of i-PPM.

where T is the symbol duration. The wave form of each symbol should have at least one event triggered due to the intensity transition that occurs at half symbol duration. In addition, if consecutive bits are identical, there would be an extra ON or OFF event. This is illustrated in Figure 3. If adjacent bits are the same (Figure 3(d) and Figure 3(c)), there would be an extra event at the boundary between two consecutive symbols. Assume that the occurrence of these four cases are uniformly distributed, the expected value of the number of generated event in one symbol duration is given by

$$\frac{1}{4} \times (1 + 1 + 2 + 2) = 1.5 \text{ (events/duration)} \quad (2)$$

Consequently, each symbol generates 1.5 events on average, which means there are

$$1.5 \times \frac{1}{T} \text{ (events/s)}. \quad (3)$$

FSK. The wave form is given by

$$s_i(t) = \text{sgn}(\cos 2\pi f_i t), 0 \leq t < T, \quad (4)$$

where s_i is the signal of the i -th symbol with frequency f_i and the symbol duration is T . This is illustrated in Figure 4. Each symbol has f_i cycles. As two events are generated in each cycle, a symbol of frequency f_i Hz would generate $\frac{2f_i}{T}$ events per symbol. Therefore, if we choose K different frequencies to represent K symbols (assume that the probability of the occurrence of these K symbols are uniformly distributed), the expected number of events per second would be

$$T \times \frac{1}{K} \sum_{i \in K} \frac{2f_i}{T} = \frac{1}{K} \sum_{i \in K} 2f_i \text{ (events/s)} \quad (5)$$

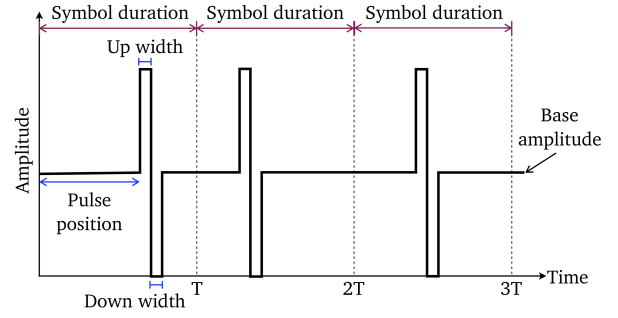


Fig. 6. The proposed new wave form.

Surprisingly, in this case, the value of symbol duration does not influence the expected number of generated events.

i-PPM. As illustrated in Figure 5, assume that the symbol duration is T , there would be two events generated per symbol. As a result, the expected number of generated events per second would be

$$2 \times \frac{1}{T} \text{ (events/s)}. \quad (6)$$

C. New wave form

In this paper, we propose a new wave form which features a large time variation (i.e., a large pulse) to increase the communication range while keeping the average luminance at a relatively low level. Figure 6 illustrates the proposed new wave form. It is similar to PPM, except that the single pulse now turns into a combination of an up pulse followed by a down pulse. This allows us to create a large falling edge while keeping the base amplitude at a desired luminance level. The large falling edge allows DVS to observe a large change of intensity, resulting in more reliable generation of events even at longer range. On the other hand, similar to PPM and i-PPM, the pulse is not perceivable by human eyes, as the duration of the pulse is very short. The idea of design a falling edge instead of a rising edge is mainly because of the finding that the OFF events are generated in a more predictable manner than the ON events (see section II).

IV. IMPLEMENTATION

Our system is composed of one DVS camera as the receiver and an OEM LED taillight as the transmitter. The output events from the DVS is collected along with a timestamp and then processed offline. As a preliminary study, all the experiments in this paper are in an indoor and static scenario, as shown in Figure 7.

A. Transmitter

At the transmitting end, a laptop instructs the Universal Software Radio Peripheral (USRP) Ettus N200 to generate modulated signals. Then, the voltage-varying signal from the USRP is converted to current-varying signals by a



Fig. 7. A view of the experimental setup: an indoor corridor in our department building.

VLC front-end board to drive the taillight, an OEM LED taillight of 2015 Toyota Corolla Altis (Taiwan model).

B. Receiver

An Inivation DVS128 is utilized as the receiver with a CS mount lens of focal length 4mm, creating an FOV of approximately 65 degree. The DVS128 has a resolution of 128x128 pixels and uses a standard USB 2.0 interface to transmit the triggered events. Each event comes with a timestamp, consisting of the location (i.e. the pixel position) of the luminance change and polarity of the intensity change. In addition, the pixel behaviors, such as response time, ON event threshold, OFF event threshold and pixel refresh time, are all adjustable by using a set of bias currents. For detailed introduction of bias settings, please refer to the support documents released by Inivation [13].

We configure the parameters of DVS such that our system can achieve longer detection (or communication) range. The output power of the taillight is configured to be the same as in usual driving scenarios. To extend the communication range, we regulate the bias setting to accommodate lower ON/OFF event threshold and to produce short response time in order to gain better performance in detecting the wave form with sharp intensity transitions at long distance.

C. Reconstruction algorithm

In this subsection, we briefly describe an algorithm to reconstruct the transmitted wave form from a series of events that DVS generates. The DVS camera is set to record the events for 100 ms. Figure 8 shows the histogram of the number of recorded events as an example. One can see that most of the events gather at certain pixels which correspond to the position of the taillight in the observed scene of the DVS128.

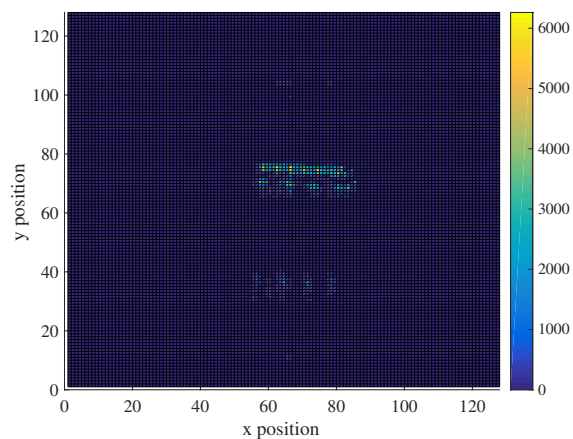


Fig. 8. An example: the histogram of the number of events recorded by DVS128.

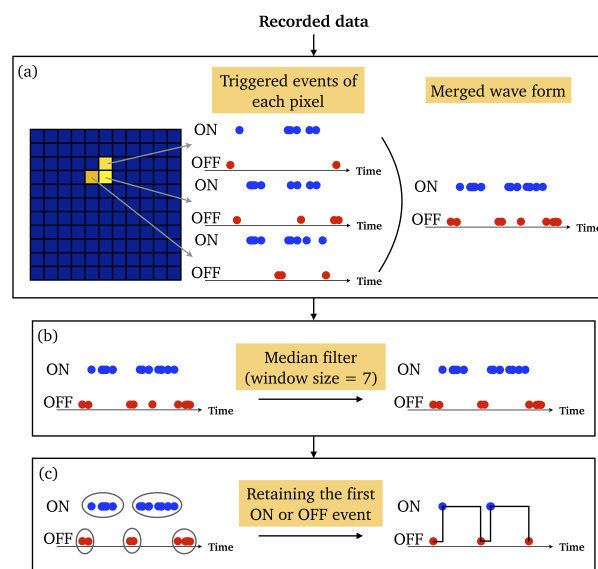


Fig. 9. An example illustrating the reconstruction process in a step-by-step manner; (a) *binning* to reduce the number of missed events; (b) median filter to mitigate shot noise; (c) segmenting and reconstruction.

A major question to be answered before designing the algorithm is *how to select the right events to rebuild the wave form*. Incorporating all recorded events for the wave form reconstruction requires too much computation. Moreover, this would include “false events” which result from internal electrical noise, as the ON/OFF event thresholds are tuned down to allow detection of small intensity changes, producing less accurate reconstruction. As a result, we retain only the events from the pixel with the largest number of events, which would likely correspond to the pixel occupied by the brightest part of the transmitting LED. On the other hand, at long distance, some events corresponding to a certain transition in the transmitted wave form would be missed. This is because the received intensity, and

therefore the difference of received intensity over time, would decrease as the distance increases, resulting in less reliable generation of events.

To address this problem, we make the following observation. Missed events in different pixels, though occupied by the same transmitting LED, are often independent. In other words, when an ON or OFF event is missed in a certain pixel, if its neighboring pixel is also occupied by the same LED, it is less likely the event is also missed in that pixel. Based on this observation, we develop a mechanism of selecting proper pixels called *binning*, as shown in Figure 9(a). First, a threshold of the minimum number of events is selected and all the events from pixels with number of events larger than that threshold are merged, and sorted according to the timestamps of the events. Then, as shown in Figure 9(b), a median filter with a window size of seven events is applied to further reduce the influence of shot noise. Subsequently, we split the sequence of events into segments of consecutive ON or OFF events, and retain only the first ON or OFF event in each segment, as shown in Figure 9(c). The timestamp of each retained event is used as the start time of the rising/falling edge of the square wave. Finally, the transmitted wave is reconstructed by filling the ON and OFF levels between the rising and falling edges accordingly.

V. EVALUATION RESULTS

A. Benchmark - Data rate versus the number of generated events

In this subsection, we evaluate how the number of generated events increases as the data rate of the system increases, both theoretically and experimentally.

Figure 10 illustrates the theoretical results making use of the formulas derived in section III-B. OOK with Manchester coding is the only scheme where the expected number of generated events increases as the data rate increases. Since OOK is a binary modulation scheme, its data rate is given by $\frac{1}{T}$. And based on Eq. 3, the expected number of generated events is proportional to the data rate.

On the other hand, the expected number of generated events of FSK, given in Eq. 5, is only proportional to the mean of all the frequencies used by the set of symbols. Our experiments reveal that square waves of frequency ranging from 4 KHz to 40 KHz can be reliably detected with an error margin of 100 Hz, if the symbol duration is set to 500 μ s. Given this frequency range and assume that the frequencies used by the symbols uniformly distributed within this range, the expected number of generated events of FSK can be given by

$$\begin{aligned} \frac{1}{K} \sum_{i \in K} 2f_i &= \frac{1}{K} * 2 * \frac{(4000 + 400000) * K}{2} \\ &= 44000 \text{ (events/s)} \end{aligned} \quad (7)$$

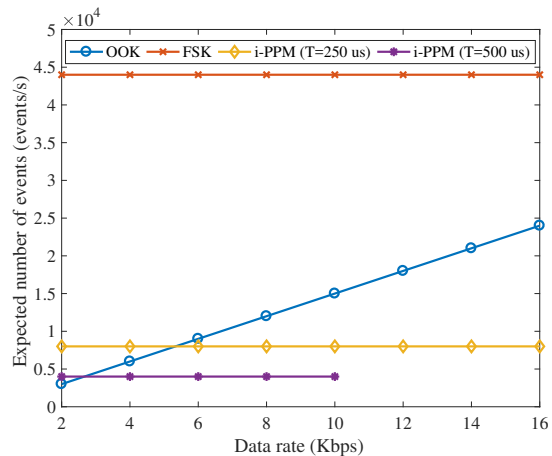


Fig. 10. Theoretical results: expected number of events versus data rate.

Counter-intuitively, the expected number is a constant and independent of the data rate² or the symbol duration T . However, the value is much higher than those of other cases, which results from the large number of intensity changes within the FSK wave form.

Finally, for i-PPM, the symbol duration is the main factor in the expected number of events (see Eq. 6). For example, the expected number of events remains at 4000 events/s when the symbol duration is 500 μ s and 8000 events/s for 250 μ s symbol duration. One can see that the maximum data rate of i-PPM with symbol duration 500 μ s stops at 10 Kbps while i-PPM with symbol duration 250 μ s can achieve a maximum data rate of 16 Kbps. This is mainly constrained by the observed pulse position error margin, which is 14.2 μ s. Throughout our experiments, we also find that the detection result is more stable when the symbol duration is 250 μ s, and thus, is used for subsequent experiments. It is worth noting that i-PPM generates the least number of events given a particular data rate.

To verify the theoretical results, we also carry out the same test experimentally with a DVS camera. Results are shown in Figure 11. One can observe that the trend of each wave form is in line with the theoretical results. However, the experimental results demonstrate higher values than the theoretical results. This might be explained as there exists not only internal electronic noise in the DVS but also ambient interference in the test environments. A similar conclusion can be drawn from the experimental results - i-PPM uses the least events given the same data rate, and thus would be used in subsequent experiments.

B. Proposed new wave form

Our proposed wave form leverages higher peak power for communication purposes, while retaining a low average

²This is under the assumption that the frequency error margin is small enough such that the given frequency range can have sufficient number of symbols (i.e., frequencies) to reach the specified data rate.

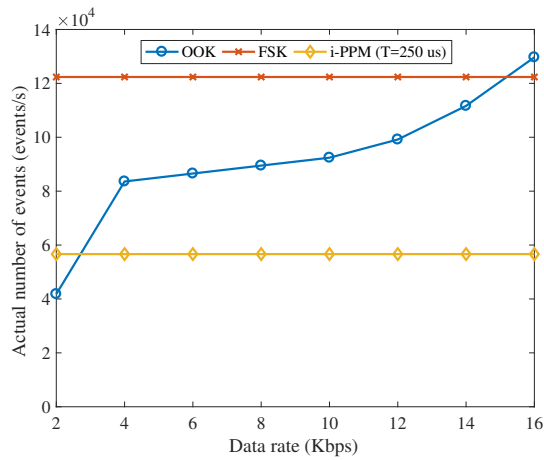


Fig. 11. Experimental results: expected number of events versus data rate.

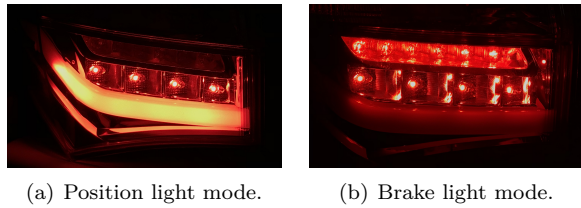
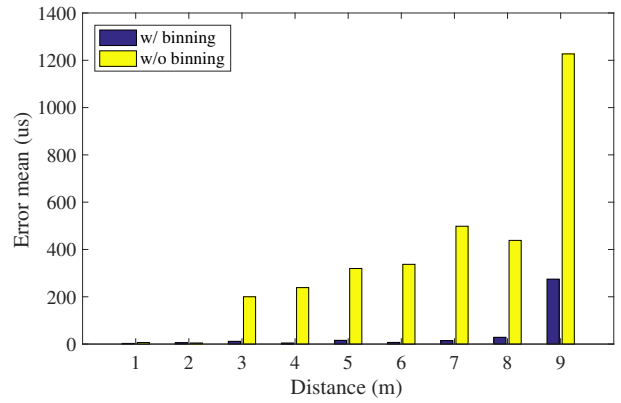


Fig. 12. Two modes of the taillight used in our implementation.

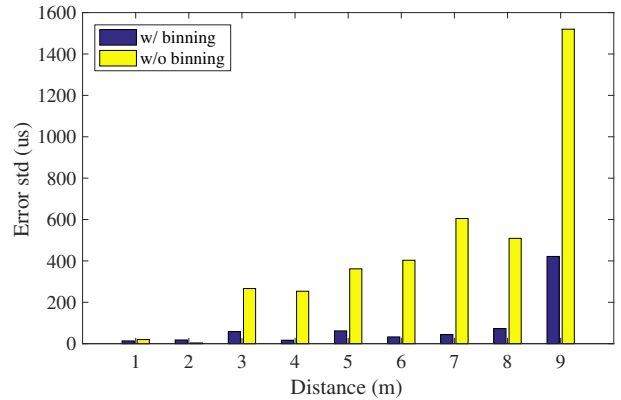
luminance level, such that it does not interfere with the illumination purpose of the transmitting LED. As the duration of the high-power pulse is very short, human eyes will only perceive constant light. In the following, we first carry out experiments to evaluate the performance of *binning* (see section IV-C), followed by a comparison of the performance of i-PPM and the new wave form.

Before we detail our experimental results, there is one thing which needs to be clarified first. The taillight used in this work can be operated in two modes: position light mode and brake light mode (hereon referred to as position light and brake light), shown in Figure 12. In order to know the performance under common driving scenarios, we are supposed to use the position light to carry out the experiments. However, the luminance of the position light cannot be driven to increase any further, and cannot be utilized by the proposed new wave form. Consequently, for the new wave form, we configure the luminance of the brake light to be reduced and as close as that of the position light in order to simulate the communication performance under a common driving scenario.

For our proposed new wave form, we set the symbol duration to be 250 μ s with a up pulse width of 16 μ s and a down pulse width of 16 μ s to achieve a maximum data rate of 16 Kbps. At the receiving end, the DVS128 camera is placed in front of the taillight at different distances. After reconstructing the transmitted wave form, the pulse positions are extracted to compare with the transmitted

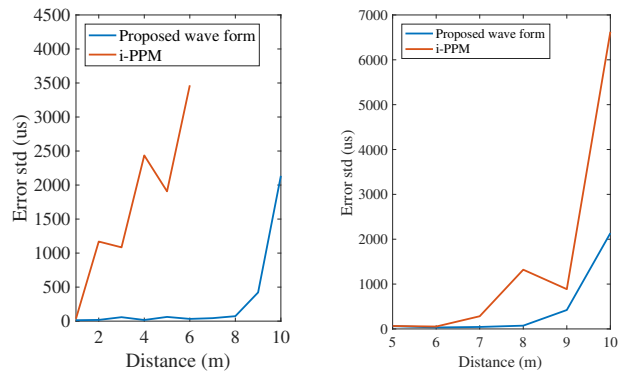


(a) Comparison of the mean of error in pulse position.



(b) Comparison of the standard deviation of error in pulse position.

Fig. 13. Comparison of system performance with and without binning.



(a) Comparisons of the proposed waveform and i-PPM using position light. (b) Comparisons of the proposed waveform and i-PPM using brake light.

Fig. 14. Comparisons of the proposed waveform and i-PPM.

pulse positions. The difference between these two values is considered as an error, and the mean and the standard deviation of the error are calculated. While we did not directly evaluate the bit error rate, a larger error in the pulse position directly corresponds to a higher error rate.

Binning. Here we would like to compare the system performance with and without *binning*. With *binning*, we set the threshold to be 60% of the largest number of events of a pixel, while in the case without *binning*, we only collect events from the pixel with the largest number of events. Figure 13 present the results. One can observe that both the mean and the standard deviation of the error significantly increase at distances larger than 3 m when *binning* is not used, while both values remain low until 9 m when *binning* is used. This provides a solid proof that applying the *binning* mechanism helps to compensate for missed events, and can effectively improve the accuracy of wave form detection.

Range. We also carried out experiments using i-PPM with both the position light and the brake light. Bias current settings are kept the same as the previous experiment. For i-PPM using position light, the average luminance is the same as the proposed new wave form. However, as shown in Figure 14(a), i-PPM using position light can only achieve approximately 3 m communication range, as the standard deviation of the error grows sharply when the distance reaches 4 m. Moreover, i-PPM with brake light, which outputs a much higher average light intensity still exhibits poorer range performance compared to the proposed new wave form. Figure 14(b) compares the standard deviation of the error for distances larger than 5 m. As one can see, despite the fact that both uses the same brake light and has an equal peak-to-peak value, the standard deviation of the error of i-PPM is larger than that of the proposed wave form at different distances.

VI. CONCLUSION

This paper presents a preliminary study to investigate the potential of using a DVS camera to implement a VLC system. From the specifications of DVS cameras and the experimental results, we showed that there are two key factors which influence the communication performance. First, the output of a DVS camera is only generated when there is a change in light intensity, and therefore the transmitted wave form should incorporate a change large enough to trigger the events in multiple pixels of the camera. Second, a DVS camera has a limitation on the maximum number of reported events, and thus the transmitted wave form should minimize its number of changes to achieve high throughput. According to our findings, we further develop a new pulse-based wave form which features a pulse with large amplitude change, while keeping the average output intensity at a low level. Our experimental results show that this new wave form is able to achieve approximately triple communication range compared to i-PPM under same average luminance level.

In this work, our implementation can reach a communication distance of 8 m, which could be sufficient for platooning, yet too short to support most of vehicular applications. Therefore, in our future work, we will first focus on extending the communication range. On other

hand, system mobility should also be included in the future work. Here, we highlight two possible problems in supporting mobility. First, a mechanism must be developed to distinguish between the events triggered by the movements and those triggered by the transmitting LED. Second, the bias setting has to be adjusted dynamically to obtain fine results at different distances, which could increase the system latency and complexity.

ACKNOWLEDGMENT

This research was supported in part by the Ministry of Science and Technology of Taiwan (MOST 107-2633-E-002-001), National Taiwan University (NTU-107L104039), Intel Corporation, and Delta Electronics.

REFERENCES

- [1] A. Cailean and M. Dimian, "Current challenges for visible light communications usage in vehicle applications: A survey," *IEEE Communications Surveys and Tutorials*, vol. 19, no. 4, pp. 2681–2703, May 2017.
- [2] A. Cailean, B. Cagneau, L. Chassagne, M. Dimian, and V. Popa, "Novel receiver sensor for visible light communications in automotive applications," *IEEE Sensors Journal*, vol. 15, no. 8, pp. 4632–4639, Aug. 2015.
- [3] N. Lourenço, D. Terra, N. Kumar, L. N. Alves, and R. L. Aguiar, "Visible light communication system for outdoor applications," in *International Symposium on Communication Systems, Networks Digital Signal Processing (CSNDSP)*, July 2012, pp. 1–6.
- [4] P. H. Pathak, X. Feng, P. Hu, and P. Mohapatra, "Visible light communication, networking, and sensing: A survey, potential and challenges," *IEEE Communications Surveys Tutorials*, vol. 17, no. 4, pp. 2047–2077, Fourthquarter 2015.
- [5] C. Danakis, M. Afgani, G. Povey, I. Underwood, and H. Haas, "Using a CMOS camera sensor for visible light communication," in *2012 IEEE Globecom Workshops*, Dec 2012, pp. 1244–1248.
- [6] H.-Y. Lee, H.-M. Lin, Y.-L. Wei, H.-I. Wu, H.-M. Tsai, and K. C.-J. Lin, "RollingLight: Enabling line-of-sight light-to-camera communications," in *Proc. of ACM Annual International Conference on Mobile Systems, Applications, and Services (MobiSys)*, 2015, pp. 167–180.
- [7] T. Yamazato, I. Takai, H. Okada, T. Fujii, T. Yendo, S. Arai, M. Andoh, T. Harada, K. Yasutomi, K. Kagawa, and S. Kawahito, "Image-sensor-based visible light communication for automotive applications," *IEEE Communications Magazine*, vol. 52, no. 7, pp. 88–97, July 2014.
- [8] I. Takai, S. Ito, K. Yasutomi, K. Kagawa, M. Andoh, and S. Kawahito, "LED and CMOS image sensor based optical wireless communication system for automotive applications," *IEEE Photonics Journal*, vol. 5, no. 5, pp. 6 801 418–6 801 418, Oct. 2013.
- [9] S. Iwasaki, C. Premachandra, T. Endo, T. Fujii, M. Tanimoto, and Y. Kimura, "Visible light road-to-vehicle communication using high-speed camera," in *2008 IEEE Intelligent Vehicles Symposium*, June 2008, pp. 13–18.
- [10] P. Lichtsteiner, C. Posch, and T. Delbruck, "A 128×128 120 dB 15μs latency asynchronous temporal contrast vision sensor," *IEEE Journal of Solid-State Circuits*, vol. 43, no. 2, pp. 566–576, Feb 2008.
- [11] "DVS and DAVIS specifications," <https://inivation.com/wp-content/uploads/2018/09/2018-09-03-DVS-Specifications.pdf>.
- [12] P. Lichtsteiner, C. Posch, and T. Delbruck, "A 128 x 128 120db 30mw asynchronous vision sensor that responds to relative intensity change," *2006 IEEE International Solid State Circuits Conference - Digest of Technical Papers*, pp. 2060–2069, 2006.
- [13] "User guide - biasing dynamic sensors," <https://inivation.com/support/hardware/biasing/>.